Corrections to Scaling in the Hydrodynamic Properties of Dilute Polymer Solutions

Burkhard Dünweg*, Dirk Reith, Martin Steinhauser, and Kurt Kremer
Max–Planck–Institut für Polymerforschung
Ackermannweg 10, D–55128 Mainz, Germany
(May 14, 2002)

We discuss the hydrodynamic radius R_H of polymer chains in good solvent, and show that the leading order correction to the asymptotic law $R_H \propto N^\nu$ (N degree of polymerization, $\nu \approx 0.59$) is an "analytic" term of order $N^{-(1-\nu)}$, which is directly related to the discretization of the chain into a finite number of beads. This result is further corroborated by exact calculations for Gaussian chains, and extensive numerical simulations of different models of good–solvent chains, where we find a value of 1.591 ± 0.007 for the asymptotic universal ratio R_G/R_H, R_G being the chain's gyration radius. For Θ chains the data apparently extrapolate to $R_G/R_H \approx 1.44$, which is different from the Gaussian value 1.5045, but in accordance with previous simulations. We also show that the experimentally observed deviations of the initial decay rate in dynamic light scattering from the asymptotic Benmouna–Akcasu value can partly be understood by similar arguments.

I. INTRODUCTION AND SUMMARY

It is well–known that the average size R of an isolated flexible uncharged polymer chain in good solvent is asymptotically proportional to N^ν, where N is the degree of polymerization, and $\nu \approx 0.5877$[1]. This law holds for any measure of the chain size, the most popular of which are the mean square end–to–end distance,

$$\left\langle R_E^2 \right\rangle = \left\langle r_{1N}^2 \right\rangle , \tag{1}$$

the mean square radius of gyration,

$$\left\langle R_G^2 \right\rangle = \frac{1}{2N^2} \sum_{ij} \left\langle r_{ij}^2 \right\rangle , \tag{2}$$

and the hydrodynamic radius

$$\left\langle \frac{1}{R_H} \right\rangle = \frac{1}{N^2} \sum_{i \neq j} \left\langle \frac{1}{r_{ij}} \right\rangle . \tag{3}$$

In these equations, we have assumed that the chain is composed of N monomers (i. e. $N-1$ bonds) at positions $\vec{r}_i$, $i = 1, \ldots, N$, and $r_{ij} = |\vec{r}_i - \vec{r}_j|$. Experimentally, the gyration radius is determined from small–angle scattering experiments; for small wave numbers q the single–chain static structure factor behaves like[2]

$$\begin{aligned} S(q) &= \frac{1}{N} \sum_{ij} \left\langle \exp\left[i\vec{q} \cdot \vec{r}_{ij} \right] \right\rangle \\ &= N \left[1 - \frac{q^2}{3} \left\langle R_G^2 \right\rangle + O(q^4) \right] . \end{aligned} \tag{4}$$

Conversely, the hydrodynamic radius is determined via small–angle dynamic light scattering experiments, where the dynamic structure factor

$$S(q,t) = \frac{1}{N} \sum_{ij} \left\langle \exp\left[i\vec{q} \cdot \left(\vec{r}_i(t) - \vec{r}_j(0) \right) \right] \right\rangle \tag{5}$$

is measured. In the small q limit, it decays like

$$\frac{S(q,t)}{S(q,0)} = \exp\left(-Dq^2 t \right) , \tag{6}$$

where D is the chain diffusion constant, which, within the framework of Kirkwood–Zimm theory[2] is related to R_H via

$$D = \frac{D_0}{N} + \frac{k_B T}{6\pi\eta} \left\langle \frac{1}{R_H} \right\rangle , \tag{7}$$

where D_0 is the monomer diffusion constant (usually this contribution is neglected), k_B is Boltzmann's constant, T the temperature and η the solvent viscosity. In principle, it is possible to obtain R_H, as a static quantity, also from purely static scattering, as is seen from the relation

$$\left\langle \frac{1}{R_H} \right\rangle = \frac{2}{\pi N} \int_0^\infty dq \left(S(q) - 1 \right) , \tag{8}$$

but for technical reasons, this has so far not been applied in experiments.

When analyzing data for the chain size, one has to take into account that the law $R \propto N^\nu$ holds only in the asymptotic limit $N \to \infty$, while for finite chain lengths deviations occur. This is particularly important for computer simulations, where data with high statistical accuracy can be obtained. For this reason, corrections to scaling have been worked out in great detail, and exploited in high–resolution numerical studies, for the end–to–end distance and the gyration radius, where the relation

*corresponding author, Electronic Mail: duenweg@mpip-mainz.mpg.de

$$\left\langle R_E^2 \right\rangle = A N^{2\nu} \left(1 + \frac{B}{N^{\Delta}} + \dots \right) \tag{9}$$

(and analogously for R_G) holds[3]. Here A and B are non–universal amplitudes, while Δ is a universal correction–to–scaling exponent, whose value is difficult to determine beyond the accuracy $\Delta \approx 0.5$ ($\Delta \approx 0.56$ according to Ref. 1, $\Delta \approx 0.43$ according to Ref. 4). The omitted terms are further powers $N^{-\Delta-1}$, $N^{-\Delta-2}$, ..., as well as $N^{-\Delta_2}$, $N^{-\Delta_2-1}$, ... (i. e. there are further larger correction–to–scaling exponents), plus so–called "analytic" terms N^{-1}, N^{-2}, ...[3]. The important point to notice is that the "analytic" corrections will arise even for a Gaussian chain, and are due to the fact that the chain consists of a finite number of beads. This will be demonstrated explicitly in Sec. II A. Conversely, the "non–analytic" corrections are due to the fact that, in the language of renormalization group (RG) theory, the chain's Hamiltonian is not identical to the fixed point Hamiltonian. The exponent Δ is related to the largest sub–leading eigenvalue of the RG transformation at the fixed point. In first order ϵ expansion its value is[5] $\Delta = \nu\omega$ with $1/\nu = 2 - \epsilon/4 + O(\epsilon^2)$ and $\omega = \epsilon + O(\epsilon^2)$, where $\epsilon = 4 - d$ and d is the spatial dimension. Higher–order calculations[6] have resulted in $\Delta = \nu\omega = 0.588 \times 0.82 = 0.482$. We adopt here the convention (which we view as quite natural) to distinguish the terms by their different origins, and call correction terms "analytic" corrections if they are present even in the Gaussian limit, while we call "non–analytic" corrections those terms which occur exclusively for excluded–volume chains. As we will see in Sec. II B, "analytic" corrections defined in this way do not necessarily imply integer powers of N.

As for the hydrodynamic radius of self–avoiding walks (SAWs), there is no high–resolution numerical study available, and corrections to scaling have not yet been dealt with systematically. This is somewhat unfortunate, since the corrections are unusually large for R_H, and of experimental relevance. For a good solvent chain, one expects again $N^{-\Delta}$ etc. terms, plus "analytic" corrections. It is the main purpose of the present paper to show that the leading–order term of these latter corrections is now given by

$$\left\langle \frac{1}{R_H} \right\rangle = \frac{A}{N^{\nu}} \left(1 - \frac{B}{N^{1-\nu}} + \dots \right), \tag{10}$$

where B is usually positive. We will show in Secs. II B and II C that this form is a straightforward consequence of discretizing the chain into beads. As $1 - \nu \approx 0.41$, this will, for long chains, ultimately dominate over the $N^{-\Delta}$ term, where the exponent is (according to Refs. 1, 4 and 6) slightly larger. Nevertheless, the exponents are so close that in most cases one will observe contributions from both terms. On the other hand, it is a well–known empirical fact that for many experimental systems, as well as for most computer models, the corrections to scaling of the gyration radius are quite weak, such that the $N^{-\Delta}$ term should have a rather small amplitude. One could therefore expect that the corresponding amplitude of the $N^{-\Delta}$ contribution in R_H is also quite small. Then the most likely candidate for explaining the experimental and numerical observation that R_H is usually subject to very large corrections to scaling[5] would actually be the "analytic" $N^{-(1-\nu)}$ term.

For a *Gaussian* chain we are able to solve the problem exactly, see Sec. II A:

$$\left\langle \frac{b}{R_H} \right\rangle = \frac{8}{3} \left(\frac{6}{\pi} \right)^{1/2} N^{-1/2} \left(1 - B N^{-1/2} + \dots \right), \tag{11}$$

with $B = -(3/4)\zeta(1/2) \approx 1.095266$ (here ζ is Riemann's zeta function), and b denoting the root mean square bond length. As $\nu = 1/2$ for a Gaussian chain, this form is consistent with Eq. 10.

The difficulties in observing the asymptotic N^{ν} scaling of R_H have a long history. Adam and Delsanti[7,8] performed dynamic light scattering experiments and found an effective power law $R_H \propto N^{0.55}$. This is quite typical, and has been found in many other experiments, too[9–11], although an exponent of 0.61[12] has been reported as well. A reduction of the effective exponent is indeed expected, as seen from Eq. 10, and is also observed in Brownian Dynamics simulations[13]. As a caveat, note that a scattering experiment does not measure R_H, but rather the diffusion constant D. This quantity has an additional D_0/N contribution (Eq. 7), which is of the same order as the leading correction of Eq. 10. Therefore, the corrections in D are weaker than those in R_H. Nevertheless, the D_0/N term is typically not large enough to fully compensate the corrections in R_H. This is easily seen for the Gaussian case from Eqs. 7 and 11: The monomer diffusion constant D_0 can be written as $D_0 = k_B T/(6\pi\eta a)$, which defines a monomer Stokes radius a. Thus

$$\frac{D}{D_0} = N^{-1} + \frac{a}{b} \left(3.6853 N^{-1/2} - 4.0364 N^{-1} + \dots \right). \tag{12}$$

Since a should be of the order of the bond length b, one sees that a large N^{-1} contribution remains.

A first attempt to explain the experimental observation is due to Weill and des Cloizeaux[14]. They conjectured that $\nu_{eff} = 0.55$ is due to non–perfect solvent quality, and a crossover between good solvent behavior ($\nu \approx 0.6$, large length scales) and Θ solvent ($\nu = 0.5$, small length scales). In particular, they pointed out that the averaging over $1/r$ assigns a very large statistical weight to the small distances. Although this latter argument is true, and generally accepted as the basic origin for the slow convergence of R_H, the explanation in terms of solvent quality has turned out to be incorrect. In Ref. 15 it was demonstrated that R_H should *not* be much more susceptible to solvent quality effects than R_E or R_G — the enhanced sensitivity of R_H to the small distances is balanced by the fact that R_E and R_G are more sensitive to

the decreased swelling of the chain near its ends: A SAW is *inhomogeneous*, i. e. $\langle r_{ij}^2 \rangle$ depends on the position of the ij bond on the chain, and is systematically larger in the interior, as has been shown both numerically[15,16] and analytically[5,15].

Furthermore, Schäfer and Baumgärtner[15] performed a detailed RG calculation and predicted in one–loop order for the universal amplitude ratio

$$\rho_\infty = \lim_{N\to\infty} \rho(N) = \lim_{N\to\infty} \frac{R_G(N)}{R_H(N)} \approx 1.06 \times \frac{8}{3\sqrt{\pi}} \approx 1.06 \times 1.5045 \approx 1.595; \qquad (13)$$

here $8/(3\sqrt{\pi})$ is the exact random walk (RW) value. Other RG studies resulted in $\rho_\infty = 1.562$[17] (this value was later revised to 1.51, see Ref. 18) and $\rho_\infty = 1.62$[19], while a semi–empirical relation based on fitting the distribution function of internal distances to light scattering data yields $\rho_\infty = 1.5955$[12,18]. A value of $\rho_\infty \approx 1.6$ was also found in Brownian Dynamics simulations[13]. From Eq. 10 it is clear that ρ should be subject to an $N^{-(1-\nu)}$ correction for finite chain length; nevertheless, experiments have so far not reported a systematic dependence on molecular weight. Typically, values around $\rho \approx 1.5$[11,12], or $\rho \approx 1.6$ / $\rho \approx 1.3$ for different solvents[10] are found in the good–solvent regime. In view of the inaccuracies of the experiments (R_G typically has an error of 5%[10]) the inability to observe a systematic behavior in N is not very surprising.

In order to contribute to the resolution of these questions, we have performed computer simulations of very different models of polymer chains, both for SAWs and for Θ chains, and calculated R_G and R_H, as outlined in Sec. III. To provide a complete and well–converged data set represents the second main goal of our paper. To our knowledge, our results are the most accurate data obtained on R_H so far. Concerning R_G, however, our data are less accurate than those of Li *et al.*[1], which we still view as the most precise numerical study on the SAW problem so far. Therefore we have taken their values for the exponents ν and Δ for our fits. We find $\rho_\infty = 1.591 \pm 0.007$ for good–solvent chains, in very good agreement with Ref. 15. (Note that our error estimate is probably overly optimistic, since it only includes statistical errors and completely neglects systematic errors.)

Theoretical and numerical investigations on corrections to scaling in R_H have first focused on the RW case. The work by Guttman *et al.*[20–22] showed by analytical calculation that a Gaussian chain should obey Eq. 11. The prefactor of the correction was first[20] determined only approximately, $B \approx 1.125$, while later[22] it was given exactly in terms of an integral. Furthermore, Monte Carlo (MC) simulations of lattice chains at the Θ point revealed that in this case the ratio R_G/R_H apparently does *not* converge to its Gaussian value 1.5045, but rather to roughly 1.4. Our simulations (see Sec. III) find a similar behavior ($\rho_\infty \approx 1.44$). We believe that this can be explained qualitatively from RG arguments[5] as follows: The asymptotic behavior is expected to be governed by the Gaussian fixed point, and thus ρ_∞, as a universal amplitude ratio, is expected to assume the Gaussian value. However, the numerical extrapolation will only produce this value if all relevant correction terms, i. e. the analytic $N^{-1/2}$ term, plus the non–analytic corrections, are consistently taken into account. Neither the data analysis by Guttman *et al.*[20,21], nor ours, fulfill this requirement, as both just fit to Eq. 10 with $\nu = 1/2$, and thus are expected to produce substantial systematic errors in ρ_∞. To do this in a better way is practically impossible, since (i) our Θ data have insufficient statistical accuracy to allow for additional fit parameters, (ii) the precise form of the correction terms is unknown for R_H (in contrast to R_E and R_G, for which the leading–order terms have been calculated by tricritical field theory[23], with the interesting feature that they are universal), and (iii) the non–analytic corrections vary extremely slowly (logarithmically) with N, such that either one would need unrealistically long chains to ensure dominance of the leading orders, or an expansion up to unrealistically high order. These problems have been elucidated in quite some detail for R_E and R_G[23], explaining previous difficulties in the interpretation of highly accurate MC data on Θ chains[24]. In this context, it should be mentioned that experiments[25,26] typically find a value of $\rho = 1.3$, i. e. a similar reduction as in the good solvent case.

Later, MC data were taken of excluded–volume (EV) chains with SAW statistics. Schäfer and Baumgärtner[15] used chains of up to 161 monomers, with an EV strength particularly close to the SAW fixed point, such that poor–solvent effects can be ruled out. The inhomogeneous swelling was demonstrated, and the R_H data were fitted with Eq. 10. This was done with an empirical correction–to–scaling exponent of $1/2$ instead of $1-\nu$. The same evidence was shown in the simulation data by Batoulis and Kremer[27] of chains of length of up to $N \approx 400$. Ladd and Frenkel[28] simulated chains of length of up to $N = 1025$ and were able to describe their R_H data via Eq. 10, with $A = 3.84$ and $B = 1.06$, but without detailed justification of their use of the correct $1-\nu$ exponent. Schäfer and Baumgärtner[15] concluded from both their analytical studies and their simulation data that not the solvent quality, but rather the chain's microstructure is responsible for the slow convergence. Our reasoning (Secs. II A–II C), which is similar to the one by Guttman *et al.*[20–22], exactly supports this picture: The corrections are due to the fact that the chain is discretized into beads, or, in other words, to the fact that there is a lower length scale cutoff for the frictional properties. However, the notion of "stiffness", which is often used in this context[15], is, in our view, somewhat misleading: As outlined in Sec. II D, we expect a large local chain stiffness to *decrease* the correction until it ultimately even changes its sign. The same conclusion has been found by Akcasu and Guttman[22] for stiff chains without excluded volume.

In the context of dynamic light scattering of dilute polymer solutions there is yet another unresolved puzzle. As Akcasu *et al.* have shown[29], the initial decay rate of the dynamic structure factor,

$$\Omega(q) = \frac{d}{dt}\frac{S(q,t)}{S(q,0)}\bigg|_{t=0}, \tag{14}$$

can be written as

$$\Omega(q) = \frac{\sum_{ij}\left\langle \vec{q}\cdot\overleftrightarrow{D}_{ij}\cdot\vec{q}\exp(i\vec{q}\cdot\vec{r}_{ij})\right\rangle}{\sum_{ij}\langle\exp(i\vec{q}\cdot\vec{r}_{ij})\rangle}, \tag{15}$$

where $\overleftrightarrow{D}_{ij}$ is the diffusion tensor. Equation 15 is a rigorous result, the only assumption being that the chain dynamics can be described by Kirkwood's diffusion equation[2]. Usually, $\overleftrightarrow{D}_{ij}$ is taken as the Oseen tensor,

$$\overleftrightarrow{D}_{ij} = D_0\delta_{ij}\overleftrightarrow{1} + (1-\delta_{ij})\frac{k_BT}{8\pi\eta r_{ij}}(\overleftrightarrow{1} + \hat{r}_{ij}\otimes\hat{r}_{ij}), \tag{16}$$

where $\hat{r}_{ij}\otimes\hat{r}_{ij}$ denotes the tensor product of the unit vector in $\vec{r}_{ij}$ direction with itself. In this case, Eq. 15 is just the $q > 0$ generalization of Eq. 7. It can then be shown[2,30] that for q in the scaling regime $R_G^{-1} \ll q \ll b^{-1}$ (b denoting the bond length), or, strictly spoken, in the limit $qb \to 0$, $qR_G \to \infty$, the relation

$$\Omega(q) = C\frac{k_BT}{\eta}q^3 \tag{17}$$

holds, where the numerical constant C only depends on chain statistics: $C = 0.0625$ for RW statistics ($\nu = 1/2$) and $C = 0.0788$ for SAWs ($\nu = 0.6$). This has been tested by light scattering experiments both for good solvents[9,12,31–33] and for Θ solvents[26,31]. In both cases the relation is verified with reasonable accuracy, but with a prefactor C which is systematically smaller than the theoretical prediction. The reasons for this shift are not clear; an attempt by a generalized theory which introduces draining[34] so far had only limited success[35]. In Sec. II E we show that the deviation can partly be explained by the fact that in reality neither $qb = 0$ nor $qR_G = \infty$ holds. Taking these nonidealities crudely into account, we find a shift in the same direction, which is however smaller than the experimental one. Nevertheless, we believe that this third main result is of direct relevance for the analysis of experimental data. There are also some indications from Molecular Dynamics simulations[36] that the description in terms of the Kirkwood theory is insufficient on these length and time scales.

II. ANALYTICAL THEORY

A. Hydrodynamic Radius of a Gaussian Chain

For a Gaussian chain with root mean square bond length b, we have

$$\langle r_{ij}^2\rangle = b^2\,|i-j| \tag{18}$$

and

$$\langle r_{ij}^{-1}\rangle = 6^{1/2}\pi^{-1/2}b^{-1}\,|i-j|^{-1/2}, \tag{19}$$

and hence

$$\langle R_E^2\rangle = b^2\,(N-1) = b^2N\left(1-\frac{1}{N}\right) \tag{20}$$

and

$$\begin{aligned}\langle R_G^2\rangle &= \frac{b^2}{N^2}\sum_{i<j}(j-i) = \frac{b^2}{N^2}\sum_{n=1}^{N-1}n(N-n)\\ &= \frac{1}{6}b^2N\left(1-\frac{1}{N^2}\right),\end{aligned} \tag{21}$$

where we have used elementary summation formulae. For the hydrodynamic radius, we find analogously

$$\langle R_H^{-1}\rangle = \sqrt{\frac{6}{\pi}}\frac{2}{bN^2}\sum_{n=1}^{N-1}n^{-1/2}(N-n). \tag{22}$$

According to the Euler–Maclaurin formula (see Appendix A), Eq. A9, the sums can be expanded as

$$\begin{aligned}\sum_{n=1}^{N-1}n^{-1/2} &= 2N^{1/2} - \frac{1}{2}N^{-1/2} + \zeta\left(\frac{1}{2}\right) + O(N^{-3/2}),\\ \sum_{n=1}^{N-1}n^{+1/2} &= \frac{2}{3}N^{3/2} - \frac{1}{2}N^{1/2}\\ &\quad + \zeta\left(-\frac{1}{2}\right) + O(N^{-1/2}).\end{aligned} \tag{23}$$

Hence,

$$\sum_{n=1}^{N-1}n^{-1/2}(N-n) = \frac{4}{3}N^{3/2} + N\zeta\left(\frac{1}{2}\right) + O(N^0) \tag{24}$$

and

$$\begin{aligned}\langle R_H^{-1}\rangle &= \sqrt{\frac{6}{\pi}}\frac{8}{3b}N^{-1/2}\times\\ &\quad\left(1 + \frac{3}{4}\zeta\left(\frac{1}{2}\right)N^{-1/2} + O(N^{-3/2})\right),\end{aligned} \tag{25}$$

which is the result anticipated in Eq. 11.

B. Hydrodynamic Radius of a Good Solvent Chain

For a linear SAW, the main difficulty is the fact that, unlike for a RW, $\langle r_{ij}^2 \rangle$ and $\langle r_{ij}^{-1} \rangle$ do *not*[5,15,16] just depend on $|i-j|$, but rather on the positions relative to the ends as well. In order to obtain the leading–order analytic corrections due to discretization, we can restrict the discussion to the leading–order scale–invariant behavior, i. e. we can assume that the SAW is strictly scale invariant with the exponent ν, with no non–analytic corrections. If we would include the latter, they would just generate further additive terms in our expressions. In what follows, we therefore omit them, for the sake of simplified notation, but keep in mind that they have to be added at the end in order to obtain the full expressions. We thus assume the relations

$$\phi_G(\lambda x, \lambda y) = \lambda^{2\nu} \phi_G(x,y), \tag{26}$$
$$\phi_H(\lambda x, \lambda y) = \lambda^{-\nu} \phi_H(x,y), \tag{27}$$

where we have introduced the notation

$$\phi_G(i,j) = \langle r_{ij}^2 \rangle, \tag{28}$$
$$\phi_H(i,j) = \langle r_{ij}^{-1} \rangle. \tag{29}$$

The definitions of R_G and R_H lead us to study the sum

$$\sigma(N) = \sum_{n=2}^{N} \sum_{m=1}^{n-1} \phi(m,n) \tag{30}$$

for $\phi = \phi_G$ and $\phi = \phi_H$, respectively, by means of the Euler–Maclaurin expansion of Appendix A. Treating the inner sum first, we find

$$\sum_{m=1}^{n-1} \phi(m,n) = \text{const.} + \varphi(n) \tag{31}$$

with the formal expansion

$$\varphi(n) = \int_1^n dx \phi(x,n) + \frac{1}{12} \frac{d}{dx} \phi(x,n) \Big|_{x=n} + \ldots, \tag{32}$$

since $\phi(n,n)$ vanishes. Note also that the constant in Eq. 31 does not depend on n, hence

$$\begin{aligned} \sigma(N) &= (N-1)\text{const.} + \sum_{n=2}^{N} \varphi(n) \\ &= (N-1)\text{const.} + \int_2^{N+1} dy \varphi(y) \\ &\quad - \frac{1}{2}\varphi(N+1) + \text{const.} + \ldots. \end{aligned} \tag{33}$$

Inserting Eq. 32, we find

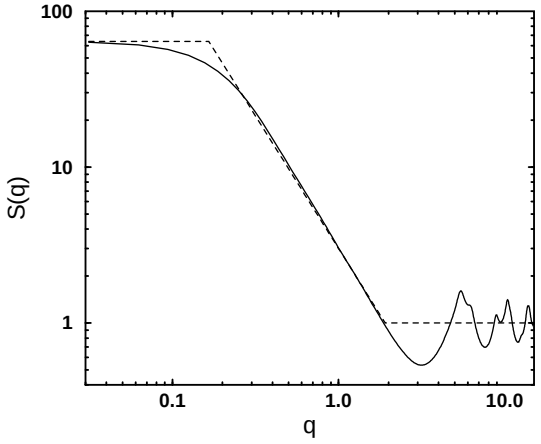

FIG. 1. $S(q)$ as defined in Eq. 4, for a chain of length $N = 64$, for model C (see Sec. III), demonstrating the $q^{-1/\nu}$ decay, followed by oscillations around unity. The dashed line is the simplified structure factor of Eq. 54.

$$\begin{aligned} \sigma(N) &= \int_2^{N+1} dy \int_1^y dx \phi(x,y) \\ &\quad + \int_2^{N+1} dy \frac{1}{12} \frac{d}{dx} \phi(x,y) \Big|_{x=y} \\ &\quad - \frac{1}{2} \int_1^{N+1} dx \phi(x, N+1) \\ &\quad + N\text{const.} \\ &\quad + \text{const.} + \ldots. \end{aligned} \tag{34}$$

After transformation to the reduced variables $u = x/N$ and $v = y/N$, and exploiting the scaling behavior of ϕ, it is possible to determine the order of each term. For the gyration radius, we find $O(N^{2+2\nu})$, $O(N^{2\nu})$, $O(N^{1+2\nu})$, $O(N^1)$, $O(N^0)$, respectively, for the five terms in order of their appearance. Conversely, for $\langle R_H^{-1} \rangle$ the different scaling behavior of ϕ implies $O(N^{2-\nu})$, $O(N^{-\nu})$, $O(N^{1-\nu})$, $O(N^1)$, $O(N^0)$ for the corresponding orders. For $\langle R_G^2 \rangle$ the leading order is $O(N^{2+2\nu})$, while the next sub–leading order is $O(N^{1+2\nu})$, resulting in a leading order correction of $O(N^{-1})$. For $\langle R_H^{-1} \rangle$, the leading order is $O(N^{2-\nu})$, followed by the $O(N^1)$ term. Thus the correction to scaling for R_H has order $O(N^{-(1-\nu)})$. This proves Eq. 10. Of course, this consideration does not prove that the amplitude B in Eq. 10 is positive; however, this is expected from the result for Gaussian chains.

C. Alternative Derivation

Equation 10 can also be derived in a more heuristic way, starting from Eq. 8. Figure 1 shows the typical behavior of $S(q)$: For wave numbers q with $R_G^{-1} \ll q \ll b^{-1}$ the structure factor exhibits a power–law decay $q^{-1/\nu}$ which indicates the chain's fractal geometry, while for larger q it oscillates around unity. We therefore can introduce a cutoff wavenumber q_0 from which on there is no

further contribution to the integral, i. e. q_0 is the smallest of all the $\hat{q}$'s with the property $\int_{\hat{q}}^{\infty} dq(S(q)-1)=0$. Hence,

$$\frac{1}{R_H} = \frac{2}{\pi N}\int_0^{q_0} dq S(q) - \frac{2q_0}{\pi N}. \tag{35}$$

It is physically clear that for a flexible chain q_0 must be roughly $(2\pi)/b$, apart from a numerical prefactor of order unity. Moreover, the fractal $q^{-1/\nu}$ decay of $S(q)$ roughly extends up to q_0, at which point $S(q)\approx 1$ is reached. We now introduce a modified structure factor $\tilde{S}(q)$, which is identical to $S(q)$ up to $q=q_0$, but extends the $q^{-1/\nu}$ decay up to $q=\infty$. In this latter regime, we have

$$\tilde{S}(q) = \alpha\left(\frac{q}{q_0}\right)^{-1/\nu}, \tag{36}$$

where α is a numerical prefactor of order unity. Therefore we can write

$$\frac{1}{R_H} = \frac{2}{\pi N}\int_0^{\infty} dq\tilde{S}(q) - \frac{2}{\pi N}\int_{q_0}^{\infty} dq\tilde{S}(q) - \frac{2q_0}{\pi N}. \tag{37}$$

Evaluating the second integral, and writing $\tilde{S}(q)$ in scaling form,

$$\tilde{S}(q) = Ns(qR_G) \tag{38}$$

(here we have again assumed strict scale invariance, i. e. absence of non–analytic corrections to scaling, for the same reason as outlined at the beginning of the previous subsection), one finds

$$\frac{R_G}{R_H} = \frac{2}{\pi}\int_0^{\infty} dxs(x) - \frac{2}{\pi}\left(\alpha\frac{\nu}{1-\nu}+1\right)\frac{q_0R_G}{N}, \tag{39}$$

i. e. again a negative correction of order $O(N^{-(1-\nu)})$.

D. Effect of Chain Stiffness

The advantage of the approach of the previous subsection is that it can be easily generalized to study the influence of local structure, since it is well–known how this is reflected in $S(q)$. For a locally stiff chain with a persistence length large compared to the bond length b, one expects that q_0 is roughly unchanged with respect to the flexible case. However, the $q^{-1/\nu}$ decay does no longer extend down to $q\approx q_0$, but only to $q\approx q_1$, where q_1 is a crossover wave number, whose inverse is a typical length scale below which stiffness effects are important. With $\tilde{S}(q)$ being again the continuation of the $q^{-1/\nu}$ decay up to $q=\infty$, we have

$$\frac{1}{R_H} = \frac{2}{\pi N}\int_0^{\infty} dq\tilde{S}(q) - \frac{2}{\pi N}\int_{q_1}^{\infty} dq\tilde{S}(q) + \frac{2}{\pi N}\int_{q_1}^{q_0} dq S(q) - \frac{2q_0}{\pi N}. \tag{40}$$

We now assume

$$\tilde{S}(q) = \alpha\frac{q_0}{q_1}\left(\frac{q}{q_1}\right)^{-1/\nu} \tag{41}$$

for $q>q_1$, and

$$S(q) = \beta\left(\frac{q}{q_0}\right)^{-1} \tag{42}$$

for $q_1<q<q_0$. Here, α and β denote prefactors of order unity, and the q^{-1} decay results from the local stretching. Evaluating the integrals, and using Eq. 38, one thus finds

$$\frac{R_G}{R_H} = \frac{2}{\pi}\int_0^{\infty} dxs(x) - \frac{2}{\pi}\left(\alpha\frac{\nu}{1-\nu}+1-\beta\ln\frac{q_0}{q_1}\right)\frac{q_0R_G}{N}. \tag{43}$$

In order to compare with the flexible case, we still have to take into account that stiffness tends to increase the gyration radius, by roughly a factor of $(q_0/q_1)^{1-\nu}$:

$$\frac{R_G}{R_H} = \frac{2}{\pi}\int_0^{\infty} dxs(x) - \frac{2}{\pi}\left(\frac{q_0}{q_1}\right)^{1-\nu}\left(\alpha\frac{\nu}{1-\nu}+1-\beta\ln\frac{q_0}{q_1}\right)\frac{q_0R_G^{(0)}}{N}, \tag{44}$$

where $R_G^{(0)}$ denotes the gyration radius in the flexible case.

The prefactor of the correction term hence depends on the stiffness parameter q_0/q_1 in a non–trivial way; for small q_0/q_1 both an increase and a decrease are possible, depending on the parameters. For sufficiently large stiffness one always obtains a decrease of the correction, and ultimately even a change of its sign.

E. Initial Decay Rate

In this subsection, we are concerned with the initial decay rate $\Omega(q)$, see Eq. 15. Splitting the sum in the numerator into diagonal and off–diagonal terms, one finds

$$\Omega(q) = \frac{D_0q^2}{S(q)} + \frac{1}{NS(q)}\sum_{i\neq j}\left\langle \vec{q}\cdot\overleftrightarrow{D}_{ij}\cdot\vec{q}\exp(i\vec{q}\cdot\vec{r}_{ij})\right\rangle. \tag{45}$$

Following Refs. 2, 37, we use the Fourier representation of the Oseen tensor for the off–diagonal elements,

$$\overleftrightarrow{D}_{ij} = \frac{k_BT}{\eta}\frac{1}{(2\pi)^3}\int d^3k\frac{\overleftrightarrow{1}-\hat{k}\otimes\hat{k}}{k^2}\exp(i\vec{k}\cdot\vec{r}_{ij}), \tag{46}$$

to find

$$\Omega(q) = \frac{D_0 q^2}{S(q)} + \frac{1}{S(q)} \frac{k_B T}{\eta} \frac{1}{(2\pi)^3} \int d^3k \times \frac{q^2 - (\hat{k}\cdot\vec{q})^2}{k^2} \left(S(\vec{k}+\vec{q}) - 1 \right). \quad (47)$$

We now focus attention on the dimensionless quantity

$$C(q) = \frac{\eta}{q^3 k_B T} \Omega(q) = \frac{1}{6\pi q a S(q)} + \frac{1}{S(q)} \frac{1}{(2\pi)^3} \int d^3k \times \frac{1 - (\hat{k}\cdot\hat{q})^2}{qk^2} \left(S(\vec{k}+\vec{q}) - 1 \right), \quad (48)$$

where we again have expressed the monomer diffusion constant D_0 in terms of a Stokes radius a. After transforming to the dimensionless integration variable

$$\vec{x} = \frac{\vec{k}+\vec{q}}{q} \quad (49)$$

and performing the angular integration, one has[2,37]

$$C(q) = \frac{1}{6\pi q a S(q)} + \frac{1}{S(q)} \frac{1}{(2\pi)^2} \int_0^\infty dx f(x) \left(S(qx) - 1 \right) \quad (50)$$

with

$$f(x) = x^2 \left(\frac{1+x^2}{2x} \ln \left| \frac{1+x}{1-x} \right| - 1 \right). \quad (51)$$

This function can be expanded as

$$f(x) = \sum_{n=0}^{\infty} \left(\frac{1}{2n+1} + \frac{1}{2n+3} \right) x^{2n+4} \quad (52)$$

for $x < 1$, and

$$f(x) = \sum_{n=0}^{\infty} \left(\frac{1}{2n+1} + \frac{1}{2n+3} \right) x^{-2n} \quad (53)$$

for $x > 1$.

In order to make further progress, we have to specify the structure factor $S(q)$. This shall be done by the most simplistic model which takes into account both finite bead size and finite chain length (see also Fig. 1):

$$S(q) = \begin{cases} N & q < \frac{2\pi}{a} N^{-\nu} \\ \left(\frac{qa}{2\pi}\right)^{-1/\nu} & \frac{2\pi}{a} N^{-\nu} < q < \frac{2\pi}{a} \\ 1 & q > \frac{2\pi}{a} \end{cases}. \quad (54)$$

We now calculate $C(q)$ in the scaling regime $R_G^{-1} \ll q \ll a^{-1}$. Defining the x values where $S(qx)$ changes its behavior as

$$x_1 = \frac{2\pi}{qaN^\nu} \ll 1, \quad (55)$$

$$x_2 = \frac{2\pi}{qa} \gg 1, \quad (56)$$

we can write $(qa)^{-1} = x_2/(2\pi)$, $S(q)^{-1} = x_2^{-1/\nu}$, $N/S(q) = x_1^{-1/\nu}$; hence

$$C(q) = \frac{1}{12\pi^2} x_2^{1-1/\nu} + \frac{1}{(2\pi)^2} x_1^{-1/\nu} \int_0^{x_1} dx f(x) + \frac{1}{(2\pi)^2} \int_{x_1}^{x_2} dx f(x) x^{-1/\nu} - \frac{1}{(2\pi)^2} x_2^{-1/\nu} \int_0^{x_2} dx f(x). \quad (57)$$

Since $x_1 \ll 1$ and $x_2 \gg 1$, we can write

$$\int_0^{x_1} dx f(x) \approx \frac{4}{15} x_1^5, \quad (58)$$

$$\int_0^{x_2} dx f(x) \approx \frac{4}{3} x_2, \quad (59)$$

where we have taken just the leading–order terms of the expansions of f; this results in

$$C(q) \approx \frac{1}{12\pi^2} x_2^{1-1/\nu} + \frac{1}{15\pi^2} x_1^{5-1/\nu} + \frac{1}{(2\pi)^2} \int_{x_1}^{x_2} dx f(x) x^{-1/\nu} - \frac{1}{3\pi^2} x_2^{1-1/\nu}. \quad (60)$$

In the asymptotic limit $qR_G \to \infty$, i. e. $x_1 \to 0$, and $qa \to 0$, i. e. $x_2 \to \infty$, this obviously converges to the asymptotic value

$$C_{as} = \frac{1}{(2\pi)^2} \int_0^\infty dx f(x) x^{-1/\nu} = \begin{cases} 1/16 & = 0.0625 \quad \nu = 1/2 \\ \sqrt{3}/(7\pi) & \approx 0.0788 \quad \nu = 3/5 \end{cases}. \quad (61)$$

Focusing now on the correction, i. e. $\Delta C(q) = C(q) - C_{as}$, we find

$$\Delta C(q) \approx \frac{1}{12\pi^2} x_2^{1-1/\nu} + \frac{1}{15\pi^2} x_1^{5-1/\nu} - \frac{1}{(2\pi)^2} \int_0^{x_1} dx f(x) x^{-1/\nu} - \frac{1}{(2\pi)^2} \int_{x_2}^{\infty} dx f(x) x^{-1/\nu} - \frac{1}{3\pi^2} x_2^{1-1/\nu}; \quad (62)$$

taking again the leading–order terms for the remaining integrals results in

$$\Delta C(q) \approx -\frac{1}{12\pi^2}\frac{3+\nu}{1-\nu}x_2^{1-1/\nu} - \frac{1}{15\pi^2}\frac{1}{5\nu-1}x_1^{5-1/\nu}. \quad (63)$$

One thus sees that *both* finite chain length *and* finite bead size have the tendency to decrease C, as observed in the experiments. The latter effect is clearly more important, as x_1 enters only via a relatively high power. Further insight is gained by numerical evaluation of the shift for reasonable parameter values.

Tsunashima *et al.*[12] performed their experiments with polyisoprene chains of size $R_G = 210nm$. Typical scattering wavenumbers in their plateau regime were given by $qR_G = 4\ldots8$; the experimental observation in this regime was $C \approx 0.06$, i. e. a shift of $\Delta C \approx -2 \times 10^{-2}$. In what follows, we consider the value $qR_G \approx 6$. Thus

$$x_2 = \frac{2\pi}{qR_G}\frac{R_G}{a} \approx 500, \quad (64)$$

where we have estimated the monomer size a as $0.45nm$[38]. Inserting this into Eq. 63, we find for the x_2 contribution a value of $\Delta C \approx -1 \times 10^{-3}$, i. e. one order of magnitude smaller than the experimental value.

It is not completely clear if a more thorough treatment of the integral would fully account for the deviation; our guess is that it would probably not. Molecular Dynamics data[36] seem to rather indicate that for typical systems (i. e. on not yet asymptotic length scales) the coupling between polymer and solvent is more complex than the simple Kirkwood description. Nevertheless, we consider our result as important for the interpretation of experimental data: There is obviously a substantial contribution to ΔC which stems from the finite bead size, and which is only weakly q–dependent. A plateau–like shape of $C(q)$ alone apparently does not guarantee asymptotic behavior. Clearly more work has to be done to fully resolve the puzzle, but we believe our considerations show that theories which neglect the influence of finite bead size (and, to a lesser degree, of finite chain length) are simply not accurate enough to describe experimental data even of rather long chains.

III. NUMERICAL RESULTS

In our numerical studies, we have used three different polymer chain models, which we will denote as model A, B, and C.

Model A is a bead–spring model in the continuum. N monomers are connected via an anharmonic ("finitely extensible nonlinear elastic") spring potential,

$$U_{FENE} = \begin{cases} -\frac{1}{2}kR_0^2 \ln\left[1-\left(\frac{r}{R_0}\right)^2\right] & r < R_0 \\ \infty & r \geq R_0 \end{cases}, \quad (65)$$

where we use the standard parameters[39] $k = 30$, $R_0 = 1.5$ in dimensionless units. Between all monomers there is an additional non–bonded potential

$$U_{LJcos} = \begin{cases} 4\left[\left(\frac{1}{r}\right)^{12} - \left(\frac{1}{r}\right)^{6} + \frac{1}{4}\right] - \lambda, & r \leq 2^{1/6} \\ \frac{1}{2}\lambda\left[\cos(\alpha r^2 + \beta) - 1\right], & 2^{1/6} \leq r \leq 1.5 \\ 0, & r \geq 1.5, \end{cases} \quad (66)$$

where α and β are determined as the solutions of the linear set of equations

$$2^{1/3}\alpha + \beta = \pi \quad (67)$$

$$2.25\alpha + \beta = 2\pi, \quad (68)$$

i. e. $\alpha = 3.1730728678$ and $\beta = -0.85622864544$. This potential has originally been constructed to simulate amphiphilic systems[40]. The parameter λ serves to control the strength of the attractive interaction and is varied instead of the temperature, which is fixed at $k_BT = 1$. For sufficiently strong λ, the chain assumes a collapsed state, while $\lambda = 0$ corresponds to good solvent. We used a combination of stochastic dynamics[39] and the pivot algorithm[3]. Applying standard methods[39] on data of chains of length of up to $N = 2000$, we located the Θ point at $\lambda = 0.65 \pm 0.02$. In the good solvent limit, and at $\lambda = 0.65$, we also ran an $N = 5000$ chain.

Model B is a mesoscopic model for an aqueous solution of the sodium salt of poly (acrylic acid) (PAA), whose input parameters have been derived from an extensive atomistic simulation of an aqueous PAA solution ($T = 333.15$ K and $p = 1$ atm) in the highly diluted regime, such that the ion concentration (number of charges on the chain, plus counterions) is 0.4 mol/l[41]. From this simulation, structural averages like the distributions of bond angles or radial distribution functions between monomers were extracted. We mapped this system to the mesoscale by replacing one repeating unit (i. e. one monomer) by one bead. As center of the coarse–grained (CG) beads, the monomer center of mass (excluding the sodium ion) was chosen. Bonded as well as non–bonded terms were parameterized by systematically varying the interactions until the structure of the atomistic model was reproduced[42]. This also allowed us to neglect all explicit water molecules and sodium ions (necessarily present in the parent atomistic simulation) in subsequent CG simulations. Their effect on the PAA chain conformation is, however, implicitly present in the model. This means that a system of roughly 10^4 atoms could be reduced to a system which consists of only 23 "super atoms". As in model A, we used both stochastic

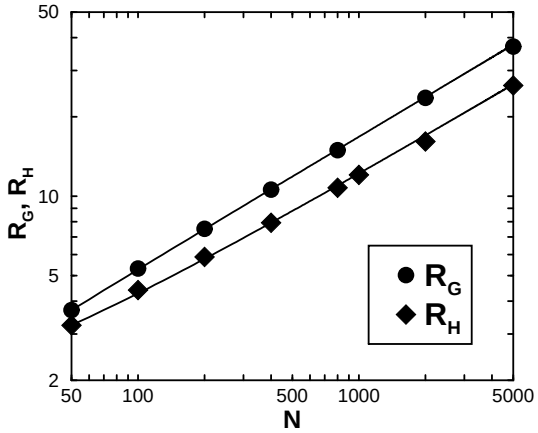

FIG. 2. $R_G = \langle R_G^2 \rangle^{1/2}$ and $R_H = \langle R_H^{-1} \rangle^{-1}$ for model A at Θ condition $\lambda = 0.65$. Error bars are smaller than symbol sizes. Also shown are the fits as discussed in the text.

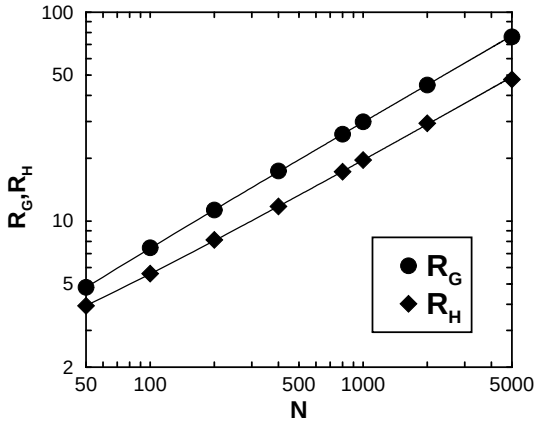

FIG. 3. Model A: Same as Fig. 2, but for good solvent condition $\lambda = 0$.

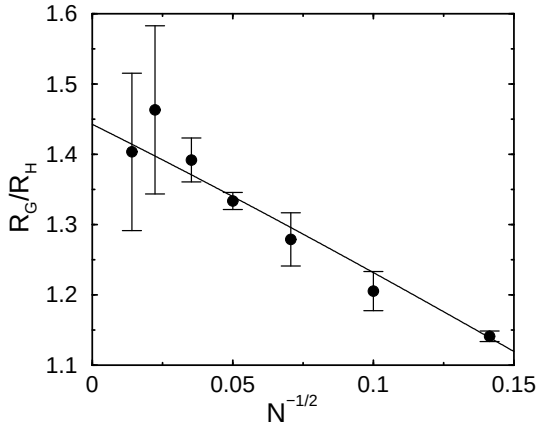

FIG. 4. Model A: R_G/R_H as a function of the scaling variable $N^{-1/2}$, at Θ condition $\lambda = 0.65$. The line results from the combined fits of R_G and R_H.

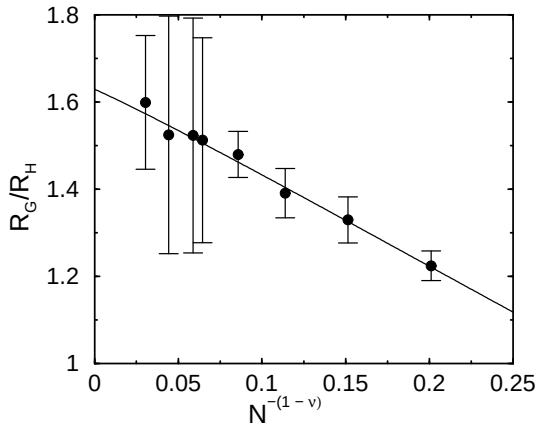

FIG. 5. Model A: R_G/R_H as a function of the scaling variable $N^{-(1-\nu)}$, at good solvent condition $\lambda = 0$. The line results from the combined fits of R_G and R_H.

dynamics and pivot Monte Carlo moves. The final force field was utilized to calculate R_G, R_H and other static properties like the structure factor for PAA strands of length 8 to 3155 repeating units[11]. The numerical results agree well with light scattering data on dilute PAA solutions with corresponding mean molar weights. In particular, the hydrodynamic radii of six different PAA–salt samples with molecular weights in the range from 18100 to 296600 g/mol were measured. For four samples, the molar masses M_W and the radii of gyration R_G were measured as well. The PAA samples were of polydispersity D_P between 1.5 and 1.8 and diluted in aqueous NaCl–containing solution $(0.1 - 1$ mol/l$)$[11].

Finally, *model C* is the SAW on the face–centered cubic lattice, which we prefer over the simple cubic for reasons of increased local flexibility, which in turn means proximity to the SAW fixed point. Units of length are defined in such a way that the bond length is $\sqrt{2}$. The chains of length $N = 64, 128, \ldots 32768$ were generated by using a dimerization procedure[3]. Up to $N = 8192$ the statistical sample always consisted of $M = 1024$ chains, while $M = 1085$ for $N = 16284$ and $M = 296$ for $N = 32768$.

In what follows, we outline our R_G and R_H data for these three models. Figures 2 and 3 summarize our results for model A at Θ condition $\lambda = 0.65$ (Fig. 2) and at good solvent condition $\lambda = 0$ (Fig. 3), respectively. For the Θ chains, we obtained very good fits with the functions $\langle R_G^2 \rangle = 0.2834N - 0.53$ and $\langle R_H^{-1} \rangle = 2.710N^{-1/2} - 3.74N^{-1}$, while for the good solvent data the analogous fits are $\langle R_G^2 \rangle = 0.2706N^{1.1754} - 0.32N^{0.62}$ and $\langle R_H^{-1} \rangle = 3.131N^{-0.5877} - 3.04N^{-1}$. These fit functions are also shown in Figs. 2 and 3. The ratio $\rho = R_G/R_H$, as it results from these data, is shown in the subsequent Figs. 4 and 5 for Θ and good solvent conditions, respectively. It should be noted that the numerical resolution (for each of our models) is clearly by far not competitive with the study by Li *et al.*[1]. For this reason, we did not attempt to determine the exponents from our data, but rather used the values for ν and Δ from Ref. 1. We did not include an $N^{-\Delta}$ term in the fit for R_H

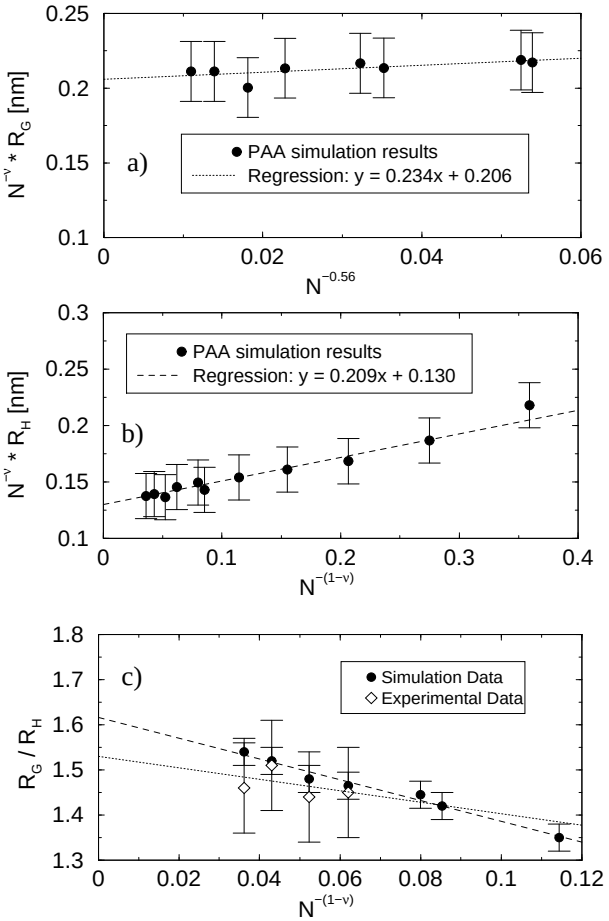

FIG. 6. Model B: Scaling behavior of poly (acrylic acid) as measured by light scattering experiments and computer simulations with a coarse–grained model: (a) Radius of gyration R_G, (b) hydrodynamic radius R_H, (c) dimensionless ratio R_G/R_H.

in the SAW case, although such a term is expected to be present. The reason is that our model A data are too inaccurate to allow for such a three–parameter fit in a stable way. Similarly, we ignored the non–analytic corrections to scaling in the Θ case, for essentially the same reason, as has been discussed in some more detail in Sec. I. Taking the statistical inaccuracies of the data, and of the resulting fit parameters into account, we obtain for the asymptotic amplitude ratio $\rho = R_G/R_H$ the values $\rho = 1.44 \pm 0.01$ at the Θ point, and $\rho = 1.63 \pm 0.01$ in the excluded–volume case. The actual error in ρ is expected to be significantly larger, since neither the uncertainties in the exponents and in the location of the Θ point, nor systematic errors due to higher–order corrections to scaling have been taken into account. This is particularly apparent in the Θ case, where one expects in the asymptotic long–chain limit rather the Gaussian value 1.5045, but also obvious in the SAW case, where the results on the longer chains of model C yield a considerably smaller value for ρ.

The most interesting aspect of model B is that it closely

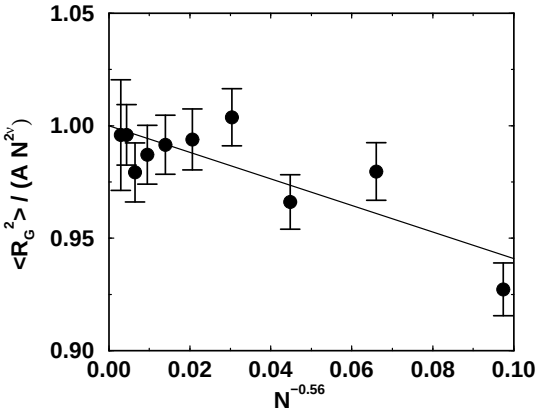

FIG. 7. Model C: $\langle R_G^2 \rangle / (AN^{2\nu})$ as a function of $N^{-\Delta}$, where we use $\Delta = 0.56$, and $A = 0.3341$ from the (also shown) fit $\langle R_G^2 \rangle = AN^{1.1754} + BN^{0.62}$.

resembles a real system, and a quantitative comparison with experiments is possible[11]. In Fig. 6 we show simulation results for R_G, R_H, and their ratio. The data are taken as published in Ref. 11. For the ratio, experimental results are also included. The scaling $N^{-(1-\nu)}$, and the extrapolation to $\rho = 1.61 \pm 0.02$ is nicely borne out by the simulation data. The experiments are too inaccurate to demonstrate a clear systematic trend. In spite of this, an extrapolation yields $\rho \approx 1.5 - 1.6$, which means that the theoretical calculations are supported by data of a real chemical system.

Our model C data (SAW) comprise the largest range of chain lengths of our three models, combined with precise estimates of statistical errors, which allows a more detailed data analysis. For our R_G data, we obtained the fit $\langle R_G^2 \rangle = AN^{1.1754} + BN^{0.62}$ with $A = 0.3341 \pm 0.0023$, $B = -0.20 \pm 0.05$, where we again use the exponents from Ref. 1. The deviation χ^2 (sum of the residuals squares, normalized by the variances) has the value $\chi^2 = 9.4$ (10 data points). The corresponding quality of fit Q, which is the probability to observe the measured χ^2 value, or a larger one, is $Q = 0.31$. Our data, in a representation which emphasizes the corrections to scaling, are shown in Fig. 7. It is seen that these are indeed weak, highlighting the difficulties in determining an accurate value for the correction–to–scaling exponent.

Turning to our R_H data from model C, we first did a nonlinear two–parameter fit $\langle R_H^{-1} \rangle = AN^{-\nu_{eff}}$, resulting in $\nu_{eff} = 0.55$. However, this fit is very poor, with a least–square sum $\chi^2 = 433$. Conversely, a linear two–parameter fit $\langle R_H^{-1} \rangle = AN^{-0.5877} + BN^{-1}$ yields a rather good value $\chi^2 = 11.8$ ($Q = 0.16$), with $A = 2.732 \pm 0.005$, $B = -3.10 \pm 0.06$, demonstrating also numerically that R_H data should be interpreted in terms of corrections to scaling, instead of an effective exponent. Actually, one should expect the presence of an additional correction of order $N^{-\Delta}$, $\Delta \approx 0.56$. Since this correction tends to decrease R_G (see Fig. 7), it should also decrease R_H, i. e. increase $\langle R_H^{-1} \rangle$, or weaken the analytic $N^{-(1-\nu)}$

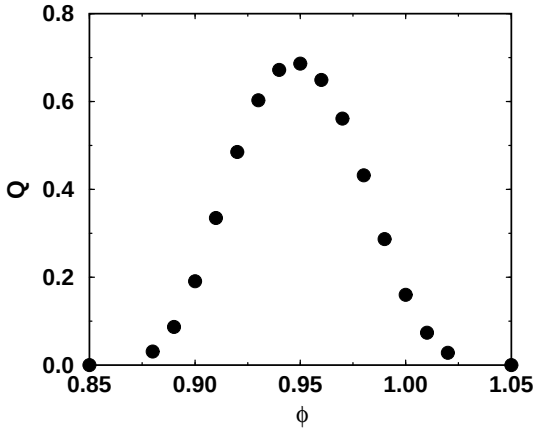

FIG. 8. Model C: Quality of the fit (see text) for the relation $\left\langle R_H^{-1} \right\rangle = AN^{-0.5877} + BN^{-\phi}$ with fixed ϕ, as a function of ϕ.

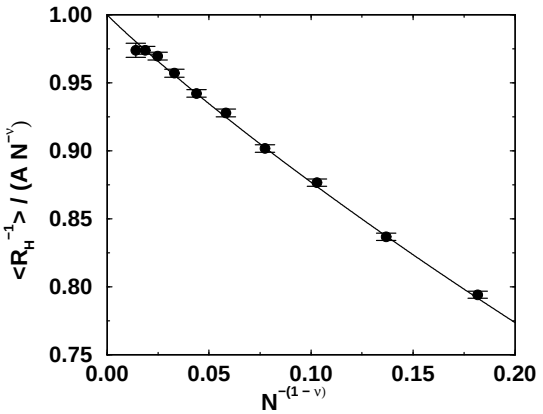

FIG. 9. Model C: $\left\langle R_H^{-1} \right\rangle / (AN^{-\nu})$ as a function of $N^{-(1-\nu)}$, where we use $A = 2.753$ from the fit $\left\langle R_H^{-1} \right\rangle = AN^{-0.5877} + BN^{-1} + CN^{-1.15}$, which is shown as well.

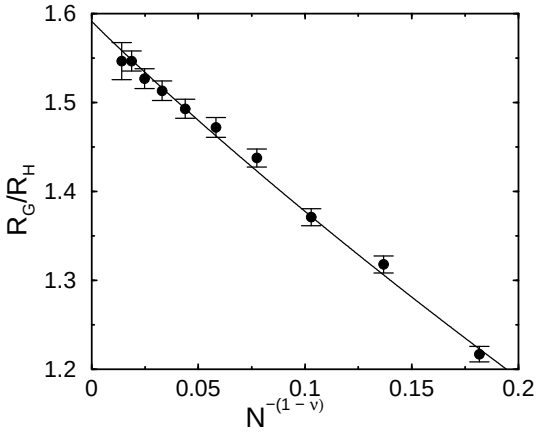

FIG. 10. Model C: R_G/R_H as a function of the scaling variable $N^{-(1-\nu)}$. The line results from the combined fits of R_G and R_H.

term. Thus, in a regression $\left\langle R_H^{-1} \right\rangle = AN^{-0.5877} + BN^{-\phi}$, where we keep ϕ fixed, one should obtain the best fit for a value of ϕ slightly smaller than unity. This is indeed what we observe, as seen from Fig. 8, where we plot the quality Q of such a fit as a function of ϕ. This figure also clearly rules out a single correction to scaling with an exponent of $1/2$ or even larger. We thus attempted a three–parameter fit $\left\langle R_H^{-1} \right\rangle = AN^{-0.5877} + BN^{-1} + CN^{-1.15}$ to also take the $N^{-\Delta}$ term into account. The result of this fit, which seems to be reasonably stable, is $A = 2.753 \pm 0.008$, $B = -4.3 \pm 0.4$, $C = 2.2 \pm 0.7$, with $\chi^2 = 5.0$, and a very good quality $Q = 0.66$. We thus use this fit to demonstrate the corrections to scaling of $\left\langle R_H^{-1} \right\rangle$ in Fig. 9, where the presence of the $N^{-\Delta}$ term shows up in a slight curvature. Finally, we also used this fit, combined with the corresponding one for R_G (see Fig. 7), to describe the data on the ratio $\rho = R_G/R_H$, as shown in Fig. 10, where the asymptotic value is 1.591 ± 0.007. Again we feel that the real uncertainty is larger, due to lack of control of the systematic errors. We also checked that both the quality of fit, and the value of ρ did not change significantly when we reduced the exponent Δ to its theoretical value[6] $\Delta = 0.482$.

To summarize, we have collected our most important numerical results, the extrapolated ρ values, in Table I.

Model	R_G/R_H
A (SAW)	1.63 ± 0.01
B (SAW)	1.61 ± 0.02
C (SAW)	1.591 ± 0.007
A (Θ)	1.44 ± 0.01

TABLE I. Asymptotic universal ratio R_G/R_H as estimated by numerical simulations of various models (see text). Error bars take into account statistical uncertainties only, while systematic errors in the extrapolation procedure are neglected.

ACKNOWLEDGMENTS

Stimulating discussions with J. Horbach, A. J. C. Ladd, J. J. de Pablo, and S. Wiegand are gratefully acknowledged. We thank L. Schäfer, A. Z. Akcasu and Y. Tsunashima for useful remarks and hints to the literature, G. Besold for a critical reading of the manuscript, and DSM and the BMBF Competence Center in Materials Simulations for financial support.

APPENDIX A: EULER–MACLAURIN FORMULA

Quite usually, sums are approximated via the corresponding integrals. The Euler–Maclaurin formula[43,44], which we outline here for the convenience of the reader, constructs a systematic asymptotic expansion around that approximation. Defining a difference operator Δ via

$$\Delta f(x) = f(x+1) - f(x), \tag{A1}$$

one obviously has

$$\Delta F(N) = f(N) \tag{A2}$$

for

$$F(N) = \sum_{n=n_0}^{N-1} f(n), \tag{A3}$$

and thus

$$F(N) = \Delta^{-1} f(N) + \text{const.}. \tag{A4}$$

On the other hand,

$$\Delta = \exp\left(\frac{d}{dx}\right) - 1 \tag{A5}$$

or

$$\begin{aligned}\Delta^{-1} &= \left(\frac{d}{dx}\right)^{-1} \left(\frac{d}{dx}\right) \left[\exp\left(\frac{d}{dx}\right) - 1\right]^{-1} \\ &= \int dx \sum_{k=0}^{\infty} \frac{B_k}{k!} \left(\frac{d}{dx}\right)^k,\end{aligned} \tag{A6}$$

where B_k are the Bernoulli numbers defined via the Taylor expansion of $x/(e^x - 1)$: $B_0 = 1$, $B_1 = -1/2$, $B_2 = 1/6$, $B_4 = -1/30$, ..., $B_3 = B_5 = B_7 = \ldots = 0$. Hence,

$$\Delta^{-1} = \int dx - \frac{1}{2} + \frac{1}{12}\frac{d}{dx} - \frac{1}{720}\left(\frac{d}{dx}\right)^3 + \ldots \tag{A7}$$

and thus

$$\begin{aligned}\sum_{n=n_0}^{N-1} f(n) = \int_{n_0}^{N} dx f(x) - \frac{1}{2} f(N) + \text{const.} \\ + \frac{1}{12}\left.\frac{d}{dx} f(x)\right|_{x=N} - \frac{1}{720}\left.\frac{d^3}{dx^3} f(x)\right|_{x=N} \\ + \ldots,\end{aligned} \tag{A8}$$

where the "integration" constant is determined via (perhaps numerical) comparison of both sides. For a power law with $q < -1$ one thus finds from the definition of the Riemann zeta function

$$\begin{aligned}\sum_{n=1}^{N-1} n^q = \frac{N^{q+1}}{q+1} - \frac{1}{2}N^q + \zeta(-q) + \frac{1}{12} q N^{q-1} \\ - \frac{1}{720} q(q-1)(q-2) N^{q-3} + \ldots.\end{aligned} \tag{A9}$$

By analytic continuation with respect to q, this result holds for general q[43].

[1] B. Li, N. Madras, and A. D. Sokal, J. Stat. Phys. **80**, 661 (1995).

[2] M. Doi and S. F. Edwards, *The Theory of Polymer Dynamics* (Clarendon Press, Oxford, 1986).

[3] A. D. Sokal, in *Monte Carlo and Molecular Dynamics Simulations in Polymer Science*, edited by K. Binder (Oxford University Press, New York, 1995), p. 47.

[4] G. Besold, H. Guo, and M. J. Zuckermann, J. Polym. Sci., Polym. Phys. **38**, 1053 (2000).

[5] L. Schäfer, *Excluded Volume Effects in Polymer Solutions as Explained by the Renormalization Group* (Springer, Berlin, 1999).

[6] J. Zinn-Justin, *Quantum Field Theory and Critical Phenomena*, 2nd ed. (Clarendon Press, Oxford, 1993).

[7] M. Adam and M. Delsanti, J. Physique **37**, 1045 (1976).

[8] M. Adam and M. Delsanti, Macromolecules **10**, 1229 (1977).

[9] N. Nemoto, Y. Makita, Y. Tsunashima, and M. Kurata, Macromolecules **17**, 425 (1984).

[10] K. Venkataswamy, A. M. Jamieson, and R. G. Petschek, Macromolecules **19**, 124 (1986).

[11] D. Reith, B. Müller, F. Müller-Plathe, and S. Wiegand, preprint, submitted to Macromolecules, cond-mat/0103329.

[12] Y. Tsunashima, M. Hirata, N. Nemoto, and M. Kurata, Macromolecules **20**, 1992 (1987).

[13] R. M. Jendrejack, M. D. Graham, and J. J. de Pablo, J. Chem. Phys. **113**, 2894 (2000).

[14] G. Weill and J. des Cloizeaux, J. Physique **40**, 99 (1979).

[15] L. Schäfer and A. Baumgärtner, J. Physique **47**, 1431 (1986).

[16] K. Kremer, A. Baumgärtner, and K. Binder, Z. Phys. B **40**, 33 (1981).

[17] Y. Oono and M. Kohmoto, J. Chem. Phys. **78**, 520 (1983).

[18] Y. Tsunashima, Macromolecules **21**, 2575 (1988).

[19] J. F. Douglas and K. F. Freed, Macromolecules **17**, 2354 (1984).
[20] C. M. Guttman, F. L. McCrackin, and C. C. Han, Macromolecules **15**, 1205 (1982).
[21] C. M. Guttman, J. Stat. Phys. **36**, 717 (1984).
[22] A. Z. Akcasu and C. M. Guttman, Macromolecules **18**, 938 (1985).
[23] J. Hager and L. Schäfer, Phys. Rev. E **60**, 2071 (1999).
[24] P. Grassberger and R. Hegger, J. Chem. Phys. **102**, 6881 (1995).
[25] M. Schmidt and W. Burchard, Macromolecules **14**, 211 (1981).
[26] Y. Tsunashima *et al.*, Macromolecules **20**, 2862 (1987).
[27] J. Batoulis and K. Kremer, Macromolecules **22**, 4277 (1989).
[28] A. J. C. Ladd and D. Frenkel, Macromolecules **25**, 3435 (1992).
[29] A. Z. Akcasu and H. Gurol, J. Polym. Sci., Polym. Phys. **14**, 1 (1976).
[30] M. Benmouna and A. Z. Akcasu, Macromolecules **13**, 409 (1980).
[31] C. C. Han and A. Z. Akcasu, Macromolecules **14**, 1080 (1981).
[32] M. Bhatt and A. M. Jamieson, Macromolecules **21**, 3015 (1988).
[33] M. Bhatt, A. M. Jamieson, and R. G. Petschek, Macromolecules **22**, 1374 (1989).
[34] Y. Shiwa, J. Phys. A, Math. Gen. **24**, L579 (1991).
[35] Y. Tsunashima, Polym. Journ. **24**, 433 (1992).
[36] B. Dünweg and K. Kremer, J. Chem. Phys. **99**, 6983 (1993).
[37] B. Hammouda and A. Z. Akcasu, Macromolecules **16**, 1852 (1983).
[38] Y. Tsunashima, private communication.
[39] K. Kremer, in *Monte Carlo and Molecular Dynamics of Condensed Matter Systems*, edited by K. Binder and G. Ciccotti (Italian Physical Society, Bologna, 1996), p. 669.
[40] T. Soddemann, B. Dünweg, and K. Kremer, Europ. Phys. J. E **6**, 409 (2001).
[41] O. Biermann *et al.*, preprint, submitted to Macromolecules, cond-mat/0101115.
[42] D. Reith, H. Meyer, and F. Müller-Plathe, Macromolecules **34**, 2335 (2001).
[43] F. W. J. Olver, *Asymptotics and Special Functions* (Academic Press, New York, 1974).
[44] R. L. Graham, D. E. Knuth, and O. Patashnik, *Concrete Mathematics* (Addison–Wesley, Boston, 1994).